Supplemental Data

PET Image Reconstruction

PET image reconstruction of both the static and the dynamic PET frames was performed using an iterative ordinary Poisson ordered subset expectation maximization (OP-OSEM) algorithm with 21 subsets and 3 iterations; the matrix was 344x344x129 and a 2-mm FWHM Gaussian post-reconstruction filter was applied. A 3D breath-hold Dixon-based MR attenuation correction map was used.

Patlak Analysis of dynamic myocardial FDG data

The Patlak graphical analysis method offers robust estimation of the net metabolic uptake rate, K_i, of FDG in the myocardium. It also accounts for the dynamic FDG activity in the blood for enhanced quantification. Injection of radiotracer whilst patients are on the MR/PET scanner is challenging because of the incompatibility of radiation shielding with the strong magnetic field of the scanner.

Therefore, patients were injected outside the scanner and immediately positioned for imaging. PET acquisition started after approximately 10 minutes. Subsequently, Patlak analysis (17) was used as it does not use dynamic tissue activity measurements $C(t_n)$ for time points earlier than $t^* = 10$ mins. However, the FDG activity concentration in the blood $C_p(t_n)$, also known as the input function (IF), of the first 10min is still needed for the calculation of its time integral from injection time. Therefore, the missing early IF section was estimated by extrapolating the measured IF section and using a model built from a retrospective population (N_{if}=20) of complete IF measurements conducted on the same scanner. The fitting of the measured IF and dynamic myocardial ROI PET data above to the Patlak model equation {1} (17) below allowed for the estimation of the myocardial FDG net uptake rate $K_i$and total blood distribution volume *V*, of which the former parameter can be used to differentiate between active cardiac sarcoid and physiological FDG uptake.

$$\frac{C(t_n)}{C_P(t_n)} = K_i \frac{\int_0^{t_n} C_p(t')dt'}{C_P(t_n)} + V, t_n > t^*, n = 1 \dots 24 \qquad \{1\}$$

Assessment of extra-cardiac sarcoid involvement

Each scan was assessed systematically for evidence of active extra-cardiac disease. Co-registered MR/PET images were interpreted in the three orthogonal planes to detect focal increased FDG uptake in different organs within the thoracic field of view (mediastinal/hilar lymph nodes, lung, liver, spleen and bone) (*Supplemental Figure 1*). The presence of active cardiac sarcoidosis was assessed in relation to the presence of active extra-cardiac sarcoidosis.

Additional information from MR/PET

Across the entire cohort evidence of active extracardiac sarcoidosis was observed in 11 (44%) patients. In the **aCS-** group, combined MR/PET with FDG identified a potential alternative cause for the cardiac symptoms in 6 (35%) patients (1 arrhythmogenic right

ventricular cardiomyopathy, 1 incidental chronic myocardial infarction, 1 aortic valve fibroelastoma, 2 anomalous coronary origins with malignant courses) (*Supplemental Figure 1*). Evidence of active extra-cardiac sarcoid disease was identified on MR/PET in 11 (44%) patients in 19 different locations, including 16 cases of lung and lymphatic involvement. It was present in 3 (38%) of the ***MR+PET+*** patients. Two previously unknown cases of sarcoid involvement in bone and in liver were also identified (*Supplemental Figure 1*).

Supplemental Figure 1. Additional Information Provided by MR/PET imaging

Active extra-cardiac sarcoidosis: **A-** Bilateral active lung sarcoidosis (arrows); **B-** Massive intra-mediastinal active LN involvement (arrows); **C-** Active sarcoid in the thoracic spine (arrow) in addition to lung involvement; **D-** Multifocal hepatic sarcoid disease (arrows).

Alternative diagnosis for the cardiac symptoms: **E-** Chronic myocardial infarction (arrows); **F-** Aortic valve fibroelastoma (arrow); **G-** Arrhythmogenic right ventricular cardiomyopathy with apical thrombus (arrow); **H-** Anomalous LAD origin with malignant course (arrow).

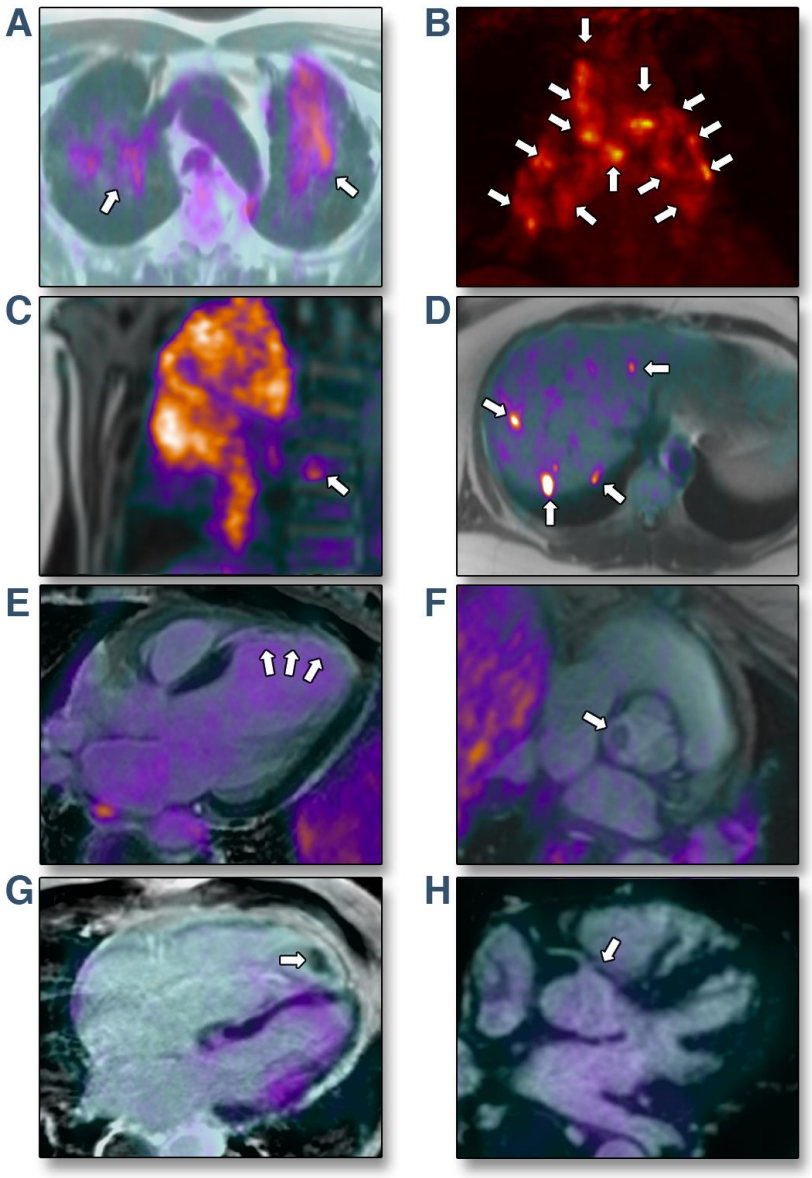

Supplemental Figure 2. False-positive myocardial FDG uptake due to failed myocardial suppression in our control group with healthy myocardium.

A- CT/PET images. Diffuse pattern (SUV_{max}=10.1, TBR_{max}=6.3 on left; SUV_{max}=12.0, TBR_{max}=7.5 on right); **B-** Focal-on-diffuse pattern localizing to the infero-lateral wall (SUV_{max}=6.4, TBR_{max}=4.0 on left; SUV_{max}=6.1, TBR_{max}=4.1 on right). Note values on CT/PET may be different to MR/PET due to differences in attenuation correction.

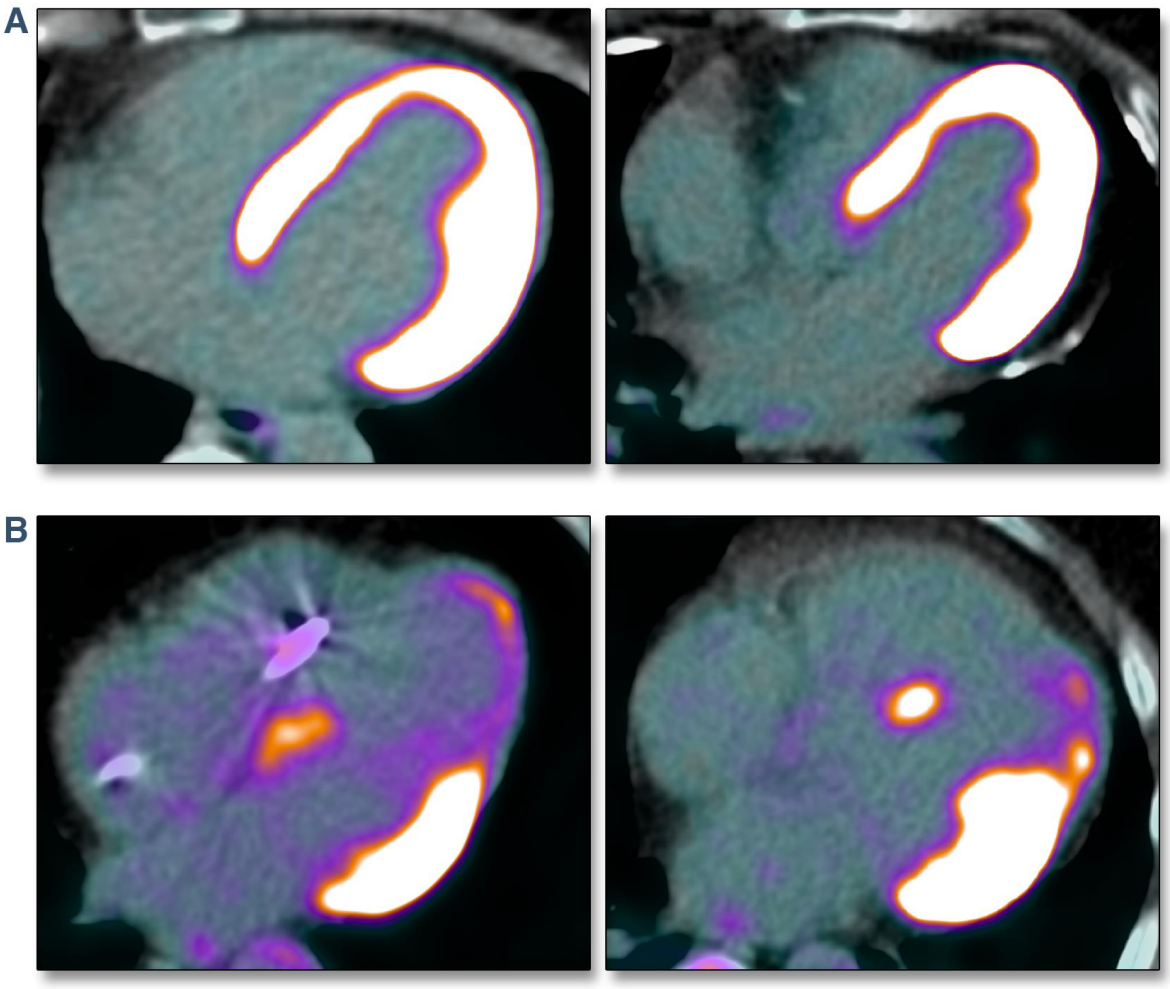
A
B